Computational Analysis of Tetrahedral Vortex Generator Effect on the Attenuation of Shock Induced Separation

Zare Shahneh A[1] (PhD, MRAeS)
Lecturer in Aircraft Design
School of Engineering, Cranfield University
United Kingdom

Abstract

The results of a computational investigation into the effects of tetrahedral sub-boundary layer vortex generator on plummeting normal shock-induced turbulent boundary layer separation are presented. The experimental work has been developed in a freestream Mach number and Reynolds number of M=1.45 and Re=15.9×10^6/m respectively. It is aimed to assess a broad band and insight observation of the phenomena by applying a rare using CFD code called STAR-CD. The control device is a pair of tetrahedral geometry vortex generator with the length of 30 mm in x direction and base sizes of 3mm in y and z directions. The device is installed at 17 times boundary layer distance upstream of shock location in the simulated transonic wind tunnel. The results are showing flow pattern in the flow field region in the form of boundary layer velocity profiles, static pressure distributions, Mach number development and surface total pressure (Preston pressure) distributions. The generally good agreement achieved in this work between the pre-assessed experimental and current CFD results opens the way for further utilization of CFD in the area of shock/boundary layer interaction with 3-D mean compressible flow field, particularly for complicated geometries and possibly the hypersonic regime as well. This will enable to reduce the experimental cost and difficulty involved in investigating such systems.

Keyword: Boundary layer, separation, normal shock wave, vortex generator, CFD, STAR-CD

1. Introduction

Above speeds of Mach 0.7, the air flowing over an aircraft wing can accelerate above the speed of sound causing a shock wave as the airplane compresses air molecules faster than they can move away from the airplane. The interaction between a turbulent boundary layer and a shock wave over the wing is a feature frequently encountered in modern aerodynamics. It can be responsible for a large loss in momentum energy. A loss of uniformity in the flow velocity and direction on a supercritical airfoil is more important than momentum loss. In the interaction zone of the shock wave boundary layer, the existence of a shock for the drag of the body is crucial as it causes separation. This phenomenon is associated with the formation of vortices and large energy losses of the body.

As already mentioned the flow speeds up as it proceeds about the airfoil, the local Mach number at the airfoil surface will be higher than the free-stream Mach number. There eventually occurs a free-stream Mach number called the critical Mach number at which a supersonic point appears somewhere on the airfoil surface, usually near the point of maximum thickness, and indicates that the flow at that point has reached Mach 1. As the free-stream Mach number is increased beyond the critical Mach number and approaches Mach 1, larger and larger regions of supersonic flow appear on the airfoil surface. When regions of subsonic and supersonic flow exist simultaneously on the surface of a body, the flow is transonic. As a transonic flow passes over the upper surface of the wing, the flow initially accelerates and therefore the surface static pressure falls. Therefore, the upper surface usually posses a large region of supersonic flow, which is terminated by a normal shock wave.

To attain the equal upper and lower pressure value at the trailing edge, by the effect of shock wave, the flow decelerates and the surface pressure rises toward the trailing edge. Transonic flow pertains to the range of speeds in which flow patterns change from subsonic to supersonic or vice versa, about Mach 0.8 to 1.2. Transonic flow presents a special problem area as neither equations describing subsonic flow nor those describing supersonic flow may be accurately applied to the regime. In order to this supersonic flow to return to subsonic flow, it must pass through a shock wave. Typical shock thickness is in the order of 0.01mm. At subsonic speeds, drag is composed of three main components: skin-friction drag, pressure drag, and induced drag (or drag due to lift).

At transonic and supersonic speeds, there is a substantial increase in the total drag of the airplane due to fundamental changes in the pressure distribution which is wave drag. The drag of the airplane wing, or for that matter, any part of the airplane rises sharply, and large increases in thrust are necessary to obtain further increases in speed. This wave drag is due to the unstable formation of shock waves that transforms a considerable part of the available propulsive energy into heat, and to the induced separation of the flow from the airplane surfaces. Throughout the transonic range, the drag coefficient of the airplane is greater than in the supersonic range because of the erratic shock formation and general flow instabilities. These shocks appear anywhere on the airplane where the localized Mach number exceeds 1.0 and the airflow must decelerate below the speed of sound. The development of transonic flow over an aerofoil can be achieved by either increasing the freestream Mach number or increasing the aerofoil incidence angle. Depending on the magnitude of Mach number, the interaction of shock boundary layer may lead to separation. It is shown that for a fixed flow incidence, flow over the wing is terminated to normal shock wave without separation up to Mach 0.78. The corresponding pressure distribution caused a steep pressure rise and thickening of the boundary layer. If the flow was inviscid the shock wave would be normal to the surface and the associate pressure rise would be predicted by the Rankine-Hugonit equation.

In this case a good recovery pressure can be achieved. A further increasing of up to Mach 0.81 has been resulted to shift forward the shock location and formation of shock induced separation. The flow will be reattached a distance downstream enclosing the region of separation. A further increasing of speed up to Mach 0.88 is resulted an extension of separation region up to the trailing edge. This also have a significant effect on the flow at the trailing edge. As previously discussed the upper and lower pressure at the trailing edge should be equal, so the upper surface pressure reduction can be achieved by an acceleration of the flow on the lower surface and hence a lower surface shock. The interaction will continue until equilibrium is established in the development of the flow. This condition is associated with unsteadiness and fluctuation called Buffeting. A further increasing of Mach over 0.92 results in both shocks moving downstream to the trailing edge and is considered as supersonic.

Numerous methods have been examined to attenuate the shock wave boundary layer separation. These methods are categorised as passive and active methods, or a combination of these known as the hybrid method. In passive methods, vortex generators have been numerously applied.

Vortex generator is a device used to delay or eliminate flow separation. Many models of vortex generators have been introduced and examined by researchers. Tetrahedral Vortex Generator first introduced by the author [1] is a promising innovation to reduce the hostile effect, which now is intended to verify by computational modelling for an insight and broad study of the physics with virtual expression of the phenomena. This paper presents the computational investigation of the control of shock induced separation by a Tetrahedral Vortex Generator using STAR-CD. The purposes of the simulation are

- To increase the confidence in the experimental results be achieving good agreement (if possible) between those results and the CFD results
- To verify the physical parameters of flow in a wide area. The experimental measurement facilities are limited in a specific area of the test section, where CFD can show the flow field physical parameters in the entire test section.
- To provide further insight into the underlying physics by obtaining and analyzing flow field behaviour that could not have been obtained using the experimental apparatus that was used in this project.
- To lay the foundation for future numerical work on this topic as is further discussed in the Conclusion Section

2. Simulation Methodology

Computational Fluid Dynamics in general is the study of a system involving fluid flow and heat transfer by numerical calculation/simulation rather than analytical and experimental approaches. The idea is to use appropriate algorithms to find solutions describing the fluid motion according to the discretized Navier-Stokes equations. It employs mathematical model in the form of a set of partial differential or integral equations and boundary conditions. The discretization is being approached by Finite Element method. Depending on the problem whether the regime is steady or unsteady state, and mostly non-linear equations needed to be applied, a method of solution can be selected.

2.1. Solution method

A level of approximation needs to be defined to obtain a desired precision. To reduce the number of degrees of freedom in the numerical solution, there are several ways which are applying to predict turbulence flows:

- By calculating the statistical average of the solution directly, called Reynolds Averaged Numerical Simulation (RANS) which is used for engineering calculations. In this model, the exact solution of velocity is split to the sum of its statistical average and a fluctuation. The fluctuation is not represented directly by numerical solution. This averaging method reduces the number of scales and therefore the number of degrees of freedom.
- By solving the Navier-Stokes equations without averaging or approximation other than numerical discretization whose errors can be estimated and controlled, called Direct Numerical Simulation (DNS). DNS can obtain accurate solution, but is very costly.
- By calculating the low frequency modes in space directly, called Large Eddy Simulation (LES). The model is based on separation of large and small scales. Cascade of large eddy to small scales is described in mechanism by Richardson in 1962 and formalized by mathematician Kolmogorov in 1941 [2]. Those scales that are greater than cut-off length are large or resolved scales, and others called small or sub-grid scale. This separation is not associated with a statistical averaging operation. Definition of cut-off length and scale separation operator are quite difficult because of numerical and modelling errors, however, on the mathematical level, the theoretical scale separation is formalized in the form of a frequency low-pass filter. The filter in the easiest approach is considered to be isotropic. It means that its properties are independent of the position and orientation of the frame of the reference in space. LES gives some relative improvements over DNS on the computational cost. In the simulation of the unsteady flow, the RANS equations based cell-centroid finite volume method is mainly used.
- By hybrid RANS/LES methods. LES has two weaknesses (the requirement to directly capture all the scales of motion, the inability for anisotropy and disequilibrium) which lead to the use of very fine mesh resolution such as the inner region of boundary layer. This method can decrease the cost of traditional LES.
- Other approaches such as calculating directly certain low frequency modes in time and the average field, called Unsteady Reynolds Averaged Numerical Simulation (URANS), Semi-Deterministic Simulation (SDS), Very Large Eddy Simulation (VLES) and sometimes Coherent Structure Capturing (CSC).

Pierre Sagaut [3] says that LES is now used as an engineering tool for several types of applications, mainly dealing with massively separated flows in complex configurations. Compressible flows quite often exhibit near-incompressible flow properties in boundary layers, once the variation of the molecular viscosity with the temperature has been taken into account, as predicted by Morkovin in his famous hypothesis in incompressible flow studying [4] ,[5]

2.2. Applied Computational Codes

Many CFD programs have been introduced for general purposes [6], [7], [8]. In the meantime, the idea of investigation of shock induced separation has been also numerically studied by simulation in CFD programs. Aktin et al [9] studied the normal shock wave / boundary layer interaction at Mach between 1.3 to 1.55 both experimental and numerical. BVGK is the one which is used to predict the effect of separation control devices. It is a transonic aerofoil code to model a passive control device. This code combines a numerical solution of the exact potential equation with integral methods for solving the boundary layer and wake equations. The code is developed for passive control aerofoil is called BVGK(P).

Recently, jBAY Vortex Generator has been investigated in Swedish Defence Research Agency [10]. jBAY is a developed and modified model of the Bender-Anderson-Yagle (BAY) model, a vane type sub boundary vortex generator. The Edge CFD flow solver was applied for the study. The first test carried out by a single vortex generator with 7mm high and 49mm long was mounted on a flat plate where the boundary layer thickness at the vortex generator location is 45mm (vortex generator height=0.16 δ). δ is the boundary layer thickness at shock location. The angle of the vortex generator to the freestream flow was 23 degrees and the speed of flow is 34m/s. The second test case was the flow through a circular duct (the RAE M2129 S-duct) and the third case was flow over a flap. An excellent agreement of CFD and experimental investigations are claimed. The model is very attractive as it is easy and simple in implementation with a high capability to predict the results.

The current study is loaned the SAR-CD code which have been used for the numerical investigation of shock induced separation of air passing sub boundary layer vortex generator in the wind tunnel.

Star-CD attributes the following specifications [11]:

- A self-contained, fully-integrated program suite comprising pre-processing, analysis and post-processing facilities
- A general geometry-modelling applicable to the complex shapes
- Extensive facilities for automatic meshing of complex geometry
- Built-in models of an extensive and continually expanding range of flow phenomena, including transients, compressibility, turbulence, heat transfer, mass transfer, chemical reaction and multi-phase flow
- Fast, easy-to-use and strong computer solution techniques that enhance reliability

The modelling process is divided into four major steps [12]: Working out a modelling strategy, setting up the flow model, performing the flow analysis and post processing the result. The vortex generator modelling in the wind tunnel can be explained briefly with the following processes:

- Producing a model and grid. A model of project is designed and is given to the system. For sub-boundary layer investigation, the flow in the wind tunnel initially is two dimensional. This is until vortex generator leading edge. The second section is the location of vortex generator. The third section is from the trailing edge of vortex generator and further. In the experiment, as many sizes and format of vortex generator located in different places are meant, therefore, these locations are not consistent.
- Input data. The main input data in addition to ambient conditions is inlet velocity which is transferred from experimental work. Wall and output conditions are also given.
- Analyzing the problem. It includes processing and graphical representation. STAR CD refers to proper equations, manipulating the solution methods and borrows them to solve the problem. It will also control the variables and desired values, monitor the numerical, boundary and cell behaviour. At any step the graphical representation is monitored.
- Output data. The results are preceded in the form of values and visualizations.

STAR-CD offers different turbulence modelling [12]: Eddy Viscosity, Reynolds Stress and Large Eddy Simulation models. In Eddy Viscosity models the well known model is based on transport equations for the turbulence kinetic energy and its dissipation rate called k-ε. High Reynolds Number k-ε model in conjunction with the law-of-the-wall represents the flow, heat and mass transfer for the near-wall region. It requires special algebraic formulae to represent the distributions of velocity, temperature, turbulence, energy, etc. within the boundary layers. The wall function representation of the near-wall turbulent behaviour is inexact, the accuracy being dependent on the assumptions and approximations.

STAR-CD also offers Reynolds Stress models, which calculate the individual Reynolds stresses directly by solving their governing transport equations. This model is able to predict complex flows more accurately than eddy viscosity models, however, several terms in the exact Reynolds stress transport equations are unknown.
It also offers the Large Eddy Simulation which is potentially a higher-level approach.

The differential equations are discretised by the finite volume approach. In fact, they are first integrated over the individual computational cells and then approximated in terms of the cell-centred nodal values of the dependent variables.

The differencing schemes applied in STAR-CD are:

- Upwind differencing (UD), the first order scheme which selects the nearest upwind
- Linear upwind differencing (LUD), the second-order accurate scheme formulated for non-structured meshes and derived from a scheme originally proposed for structured meshes
- Central differencing (CD), is also second-order, simply interpolates linearly on nearest neighbour values, irrespective of flow direction,
- Quadratic upstream interpolation of convective kinematics (QUICK), which is a third order scheme which fits a parabola through two points upstream and one point downstream to get an interpolated value
- MARS is a multidimensional second-order accurate differencing scheme, and may also be used for the calculation of density.

The current work has used all the above methods in try and error format to achieve the target. k-ε turbulent modelling is found more advantageous bearing the closed meeting with experimental.

3. Results and discussion

3.1. Baseline analysis

In the experimental investigation, all experiments have been done in a supersonic wind tunnel. The wind tunnel is simulated with the same input and boundary conditions as experimental case. It is considered a two dimensional flow regime. Fig. 1 shows the shock wave captured and Lambda form has appeared.

Based on theory, since the flow upstream of shock is supersonic, so for all gaseous with specific heat capacity greater than one, downstream Mach number should be subsonic. Also variations of pressure, density and temperature equations with Mach, it is resulted that the ratio of each of these parameters depends only on upstream Mach number for air. Fig. 2 shows that pressure and temperature are increasing across a shock wave, while the Mach number is decreasing.

Fig. 3 shows the separated area induced by boundary layer shock wave interaction commencing from the beneath of the shock location. It is quite similar to the formation of separation produced in PREPHA program, shown in Fig. 4. [13]

3.2. Flow simulation with vortex generator

Design specifications

Design of the system with a vortex generator is quite different and more complicated than baseline. A pair of Tetrahedral Vortex Generators is simulated in the wind tunnel. Numbers of blocks are drawn to provide vortex pieces geometry on the wind tunnel floor and then merged and celled. It comprises 2.26 million cells.

The length of the simulated wind tunnel in x direction is 860mm, the width in z direction is 126mm and the height in y direction varies from 130mm at inlet, increasing up to 145mm, and then changes curvedly from 145mm to 130mm and then to 148mm in a small length to produce the shock generator curve. It ended to 150mm at outlet. The vortex generator leading point is installed at x=60mm, so the trailing edge will be at x=90mm. Fig..5 shows the grid structure of the model.

The model is then refined within two attempts in the boundary layer area downstream of shock wave as is shown in Fig.6.

The main input data is the entrance velocity equal to 374m/s which increases up to shock location. Air properties in the ambient condition are other sort of input data. The perspective of wind tunnel at post processing stage is as shown in Fig.7. It shows all 3 dimensions which is followed in all further figures.

Results and descriptions

Fig. 8 shows the shock wave captured in the velocity contour, as a sharp reduction of flow velocity is occurred. The slice is the centreline along the tunnel.

Fig.9 shows relative static pressure contour zoomed at shock wave location. It illustrates a sudden increasing of pressure at shock location.

Static pressure contour across the tunnel in the area commencing by shock location to considerably far downstream shock location is almost constant.

The effect of vortex generator can be observed with velocity contour in different height slices (Fig. 10). Slice 0.0001/150, which is the first possible y-coordinate slice to the surface, shows a high variation of velocity magnitude around the vortex generator pair, which can be seen precisely in the zoomed picture as well (Fig. 11).
In Fig. 10 at 2mm above the surface downstream of vortex generator beneath the shock wave, the effect of vortex generator developed in the centreline zone. In the upper slices and at downstream of shock wave location, vortices are developed and then in the upper slices are reduced, where at slice 25mm above the surface, a very smooth effect can be observed.

Fig.12 shows two chosen slices of zoomed velocity profile at shock location zone: 1mm and 7mm above the surface. In 1mm above the surface, variation of velocity around the vortex is considerably high both before and after the vortex generator and at 7mm above the surface, a lower effect of velocity changes can be observed.

Vortex development

Streamwise slices of velocity contour can attractively demonstrate the vortices produced by a pair of vortex generators. Fig. 13 shows the whole wind tunnel and one slice of the velocity, if one stands and looks at the coming air. The whole wind tunnel length is 860 mm, however, slices after shock position to 200mm downstream are concerned.

A few chosen figures of velocity contour slices are shown in Figs 14 to 18. Fig.14 shows a streamwise slice of velocity contour at the leading edge of vortex generator. The top figure shows the whole wind tunnel cross section, where it zoomed at the vortex position and is shown in the bottom. This figure illustrates that velocity near the vortex decreases and pressure increases as the flow faced an obstacle. Velocity variation from wind tunnel surface to the top shows a velocity rise upward as it is expected, however, a difference with experimental work can be found. In experimental work, boundary layer thickness stands at 99.5% of freestream, and above that, it is considered a constant freestream velocity. The Fig. 14 shows that variation of velocities from blue colour up to red colour which is at the location of half of the wind tunnel height is slowly. In fact velocity gradient across the wind tunnel for the thickness of 99.5% to 100% is very low but not zero or variation from 99.5% to 100% occurs in a thick layer upward. The velocity near the top of the tunnel again decreases which clearly shows top surface of tunnel and a boundary layer formed there. The difference between up and down spectrum can be explained by the effect of vortex device mounted on the surface.

The sizes of this zoomed picture are kept constant for the rest of pictures. Fig. 15 shows the velocity contour of the vortex trailing edge slice. The picture shows the proper generation of vortices. There are two counter-rotating vortices formed at this point. The contour table shows a decreasing velocity changes from the centre point of each vortex outward.

Fig. 16 shows the formation of vortices at 10mm, 20mm and 60mm downstream of vortex location. It shows the development of counter-rotating vortices created by the vortex generator. As they progress, they merge to each other; producing a merged form of vortex shown consequently in 90mm and 140mm downstream vortex generator shown in Fig. 17. The bottom picture of this figure shows the exact position of the vortex generator in the entire tunnel cross section. It is clearly shown that the location of vortex moved upward. However, in this section, the flow is affected by shock generator and made another spectrum of velocity variation (Fig. 18), in comparison with the section upstream shock wave (Fig. 14a).

Vortex specifications

Beyond the development of vortices along the wind tunnel, the views of velocity vectors around a vortex show clearly the magnitude and the direction of flow. Fig. 19 shows the velocity vectors zoomed around a vortex 10mm and 13mm downstream of vortex generator trailing edge. At these sections, a clockwise rotation of flow can be observed where flow at the centre point of vortex is low and increases by radius where the flow near the surface is quite high.

3.3. Comparison between Experimental and CFD results

Total pressure

The outcome of CFD streamwise surface total pressure at the centreline is compared with the experimental results and is shown in Fig. 20. The resultant difference is low and so the outcome is satisfactory.

Static pressure

Pressure distribution along the wind tunnel for both experimental and CFD investigations show a considerably well meeting (Fig. 21). The incompatibility of the points upstream shock wave are quite high, but close to shock wave location through the downstream becomes lower.

Mach number

The position of shock wave captured in the simulated wind tunnel in comparison with the experiment has an error of 2.5% (based on ratio of the difference between shock location and vortex generator location of experiment and CFD over the distance in experiment).

Considering this low difference, the Mach number of experiment and CFD are shown in Fig.22. It shows a quite good agreement of the Mach number of experiment with CFD at the zone of shock wave, where the point behind the shock location has large difference, but at the area of shock wave location and downstream has a very good agreement.

4. Conclusion

Simulation of a pair of Tetrahedral Vortex Generator in a supersonic wind was performed for flow parameters matching a reference experiment showed the possibility of an accurate numerical prediction of a shock wave/turbulent boundary layer interaction. The shock wave position according to the numerical prediction was only 2.5% away from the experimental finding (that ratio is defined as the difference between shock location and vortex generator location of experiment and CFD over the distance in experiment). The numerical calculation also clarified the effects of the shock wave on the static pressure, total pressure and Mach number distributions. Velocity contours at different stream-normal slices demonstrated the variation of velocity, showing a decrease in the velocity upstream of the vortex generator as it faced a high pressure zone on the obstacle, and a jet flow downstream of the vortex generator location. Velocity contours in streamwise slices showed counter-rotating vortices that evolved along the wind tunnel. The flow analysis showed that three-dimensional effects inside the boundary layer started from the upstream vortex location and progressed up to 400mm downstream of shock wave location. This finding imposes new requirements for any future planned experiment.

The experimental and CFD results for static pressure, surface total pressure and Mach number distributions showed generally good agreements that could have been enhanced by further stages of grid refinements in CFD calculation. Nevertheless, they did not show fine detail agreement at a zone upstream of shock location. Velocity vector analysis downstream of vortex generator confirmed the transportation of momentum into the boundary layer, where the resultant vortices could energize the near wall area. The distribution of surface total pressure along the wind tunnel showed that CFD results were compatible with experimental and therefore attenuation of separation was confirmed.

The generally good agreement achieved in this work between the experimental and CFD results opens the way for further utilization of CFD in the area of shock/boundary layer interaction with 3-D mean compressible flow field, particularly for complicated geometries [14] and possibly the hypersonic regime as well. This will enable to reduce the experimental cost and difficulty involved in investigating such systems.
The results of the CFD also can facilitate the future work by the following objectives:

- To find the effect of a single parameter by isolation a specific parameter.
- To facilitate a change in a parameter and giving great visual results in a relatively short time
- To develop and optimize the different models and configurations

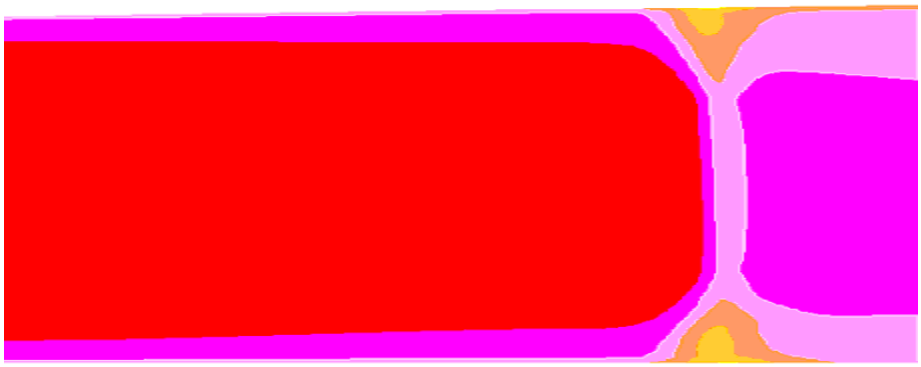

Fig. 1. Formation of shock wave and Lambda in a simulated supersonic wind tunnel

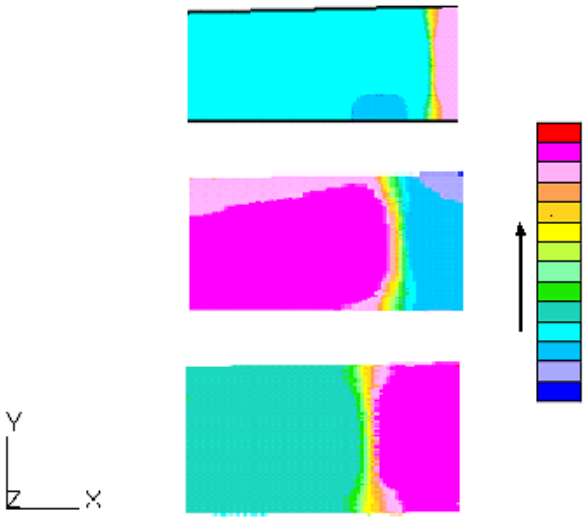

Fig. 2. Effect of shock wave on the fluid properties. Top: static pressure increases, middle: Mach number decreases, bottom: temperature increases. The contour is on the right side, shows value increasing from bottom to top.

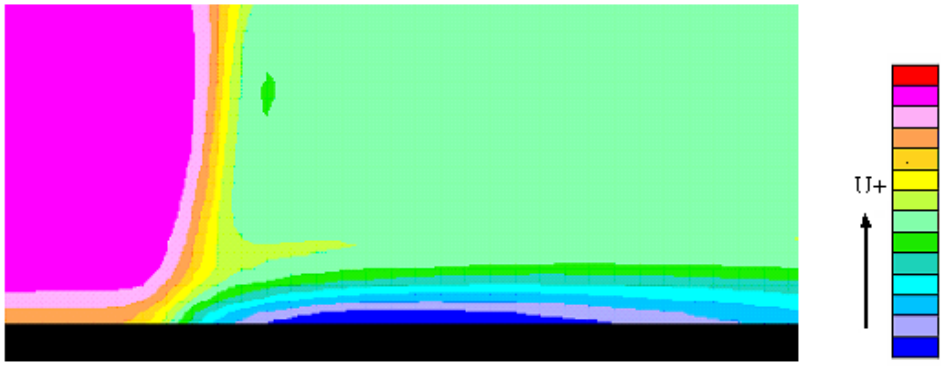

Fig. 3. Separated flow beneath the shock wave. Contour shows velocity rise direction.

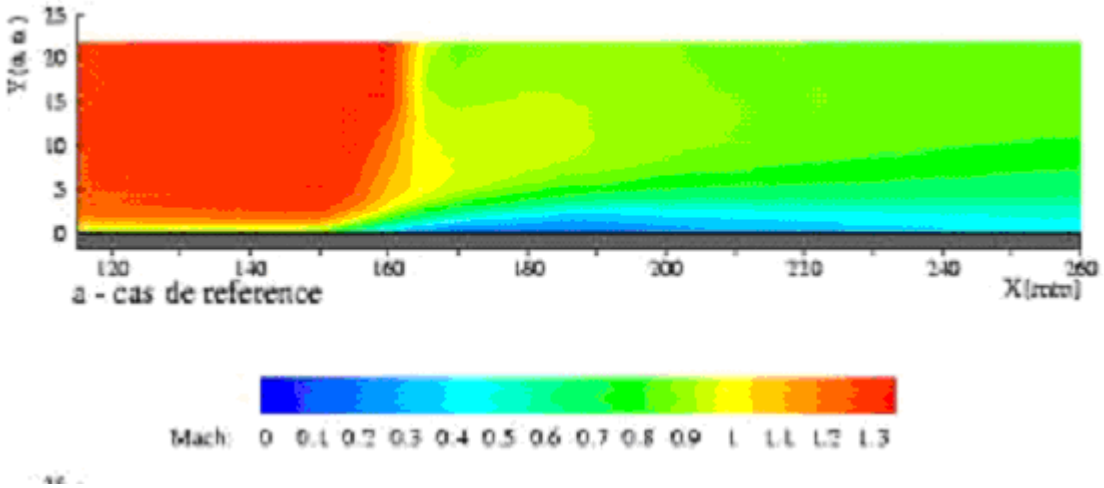

Fig. 4. Shock wave and separation produced in PREPHA program [13]

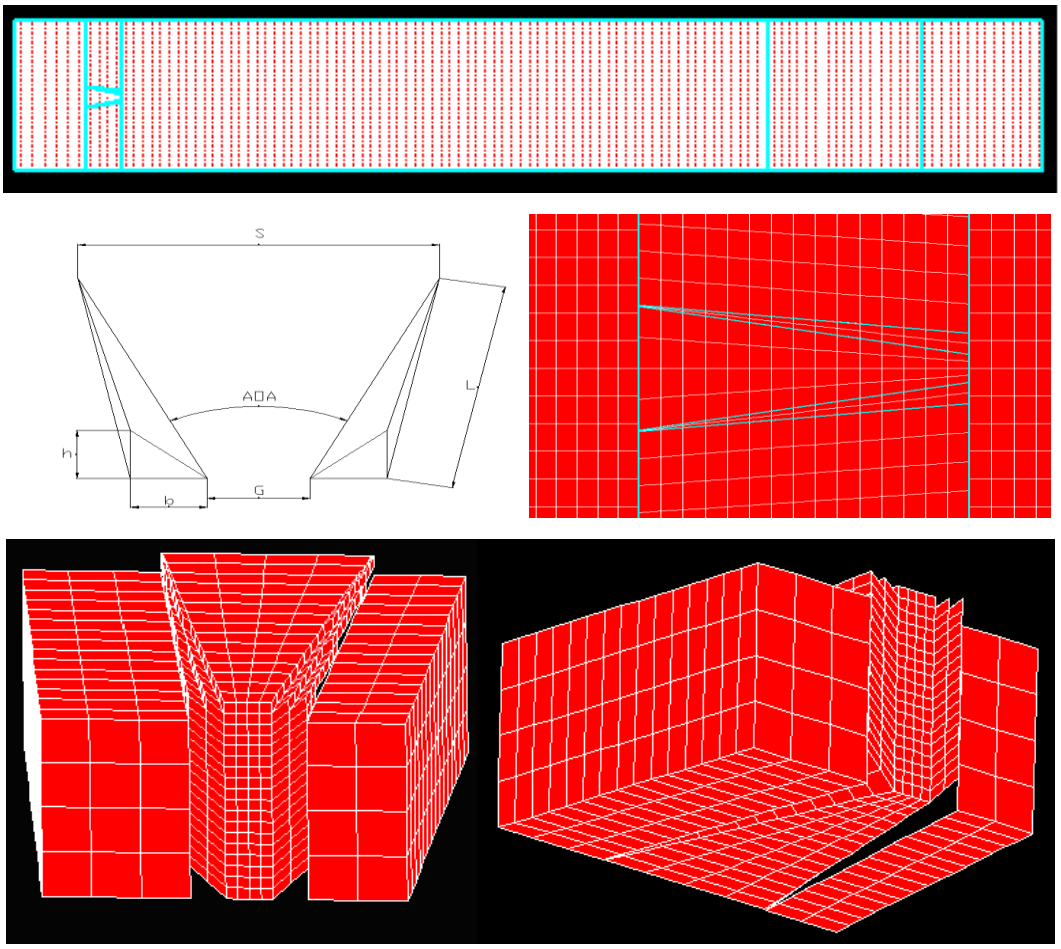

Fig. 5. Block structured cells of the wind tunnel with vortex generator. Top: top view of the whole tunnel; middle left: schematic of vortex generator; middle right: top view zoomed at vortex generator location; bottom: a section of vortex generator pair viewed from the front and the bottom 3 dimensionally.

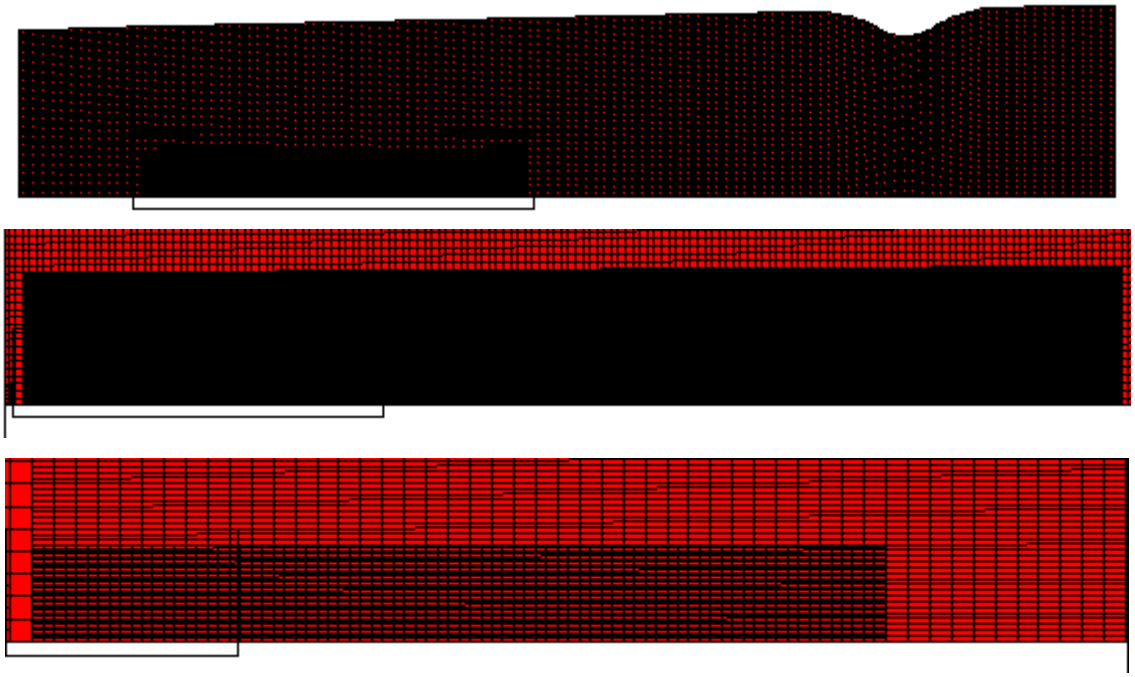

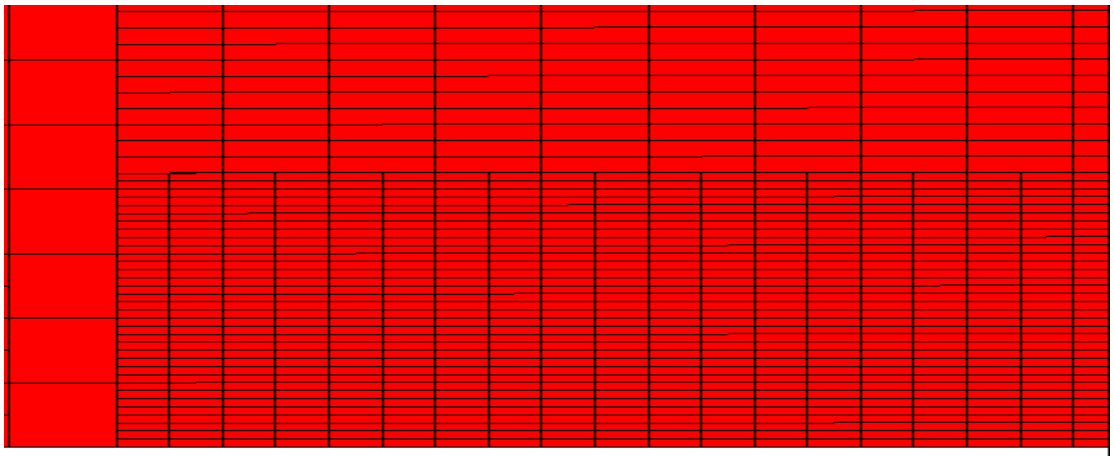

Fig. 6. Refinements of boundary layer zone, zoomed from the whole wind tunnel on the top to the bottom

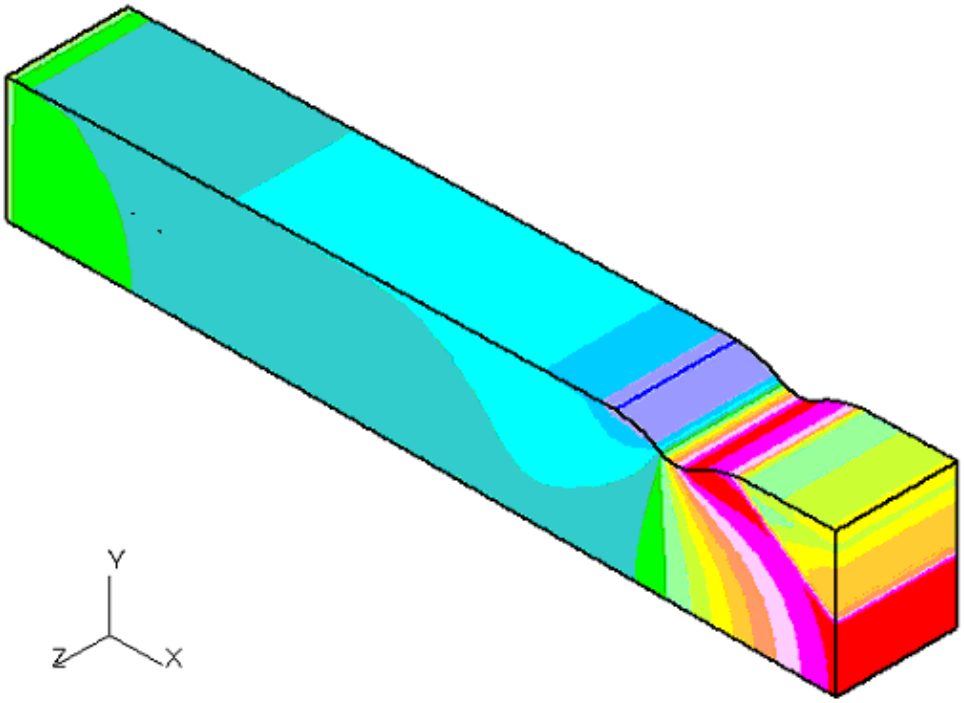

Fig. 7 . Perspective of simulated wind tunnel

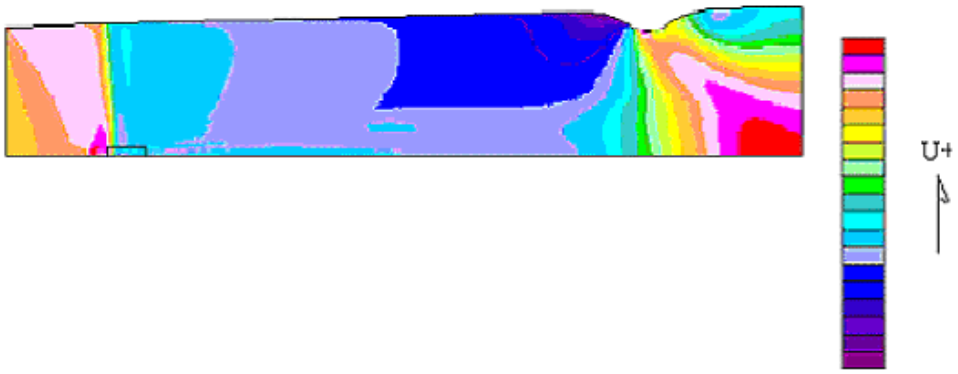

Fig. 8. Velocity contour at centreline along the test section

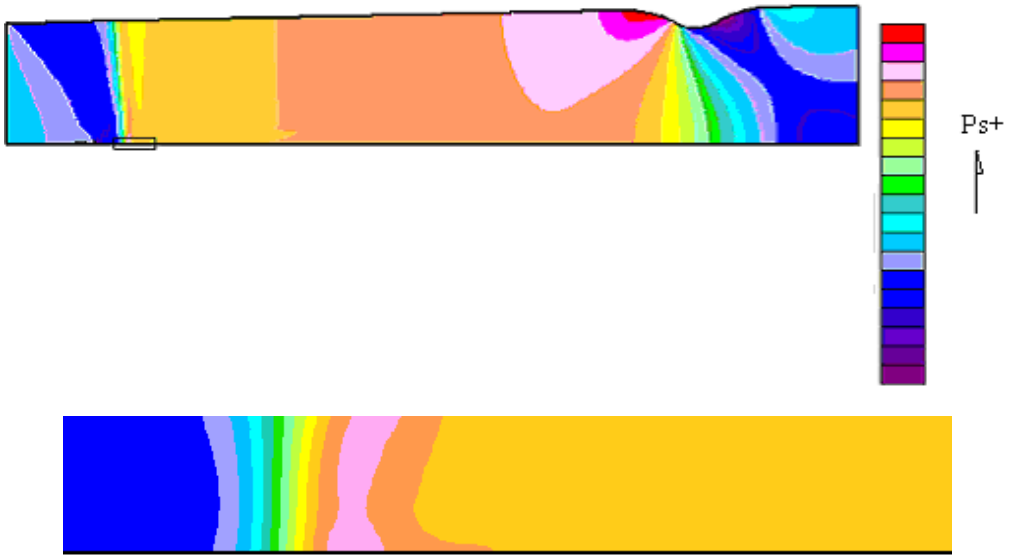

Fig. 9. Relative static pressure contour at centreline, above: along the wind tunnel, bottom: zoomed at shock wave location

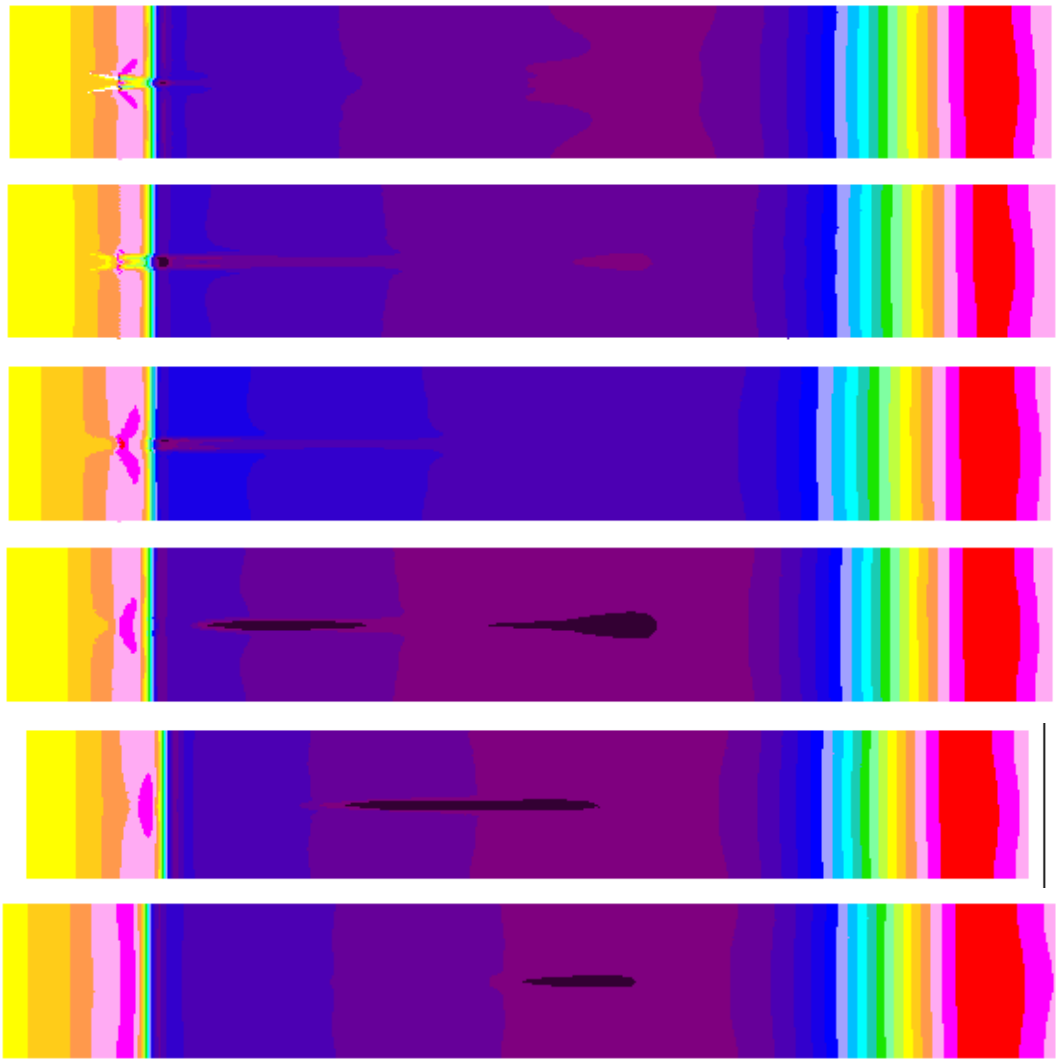

Fig. 10. Top view of velocity contour at different slices in y-coordinate. From the top are slices 0.0001/150(at the surface), 2mm, 4mm, 8mm, 15mm and 25mm above the surface. The contour colour variation is as Fig. 8.

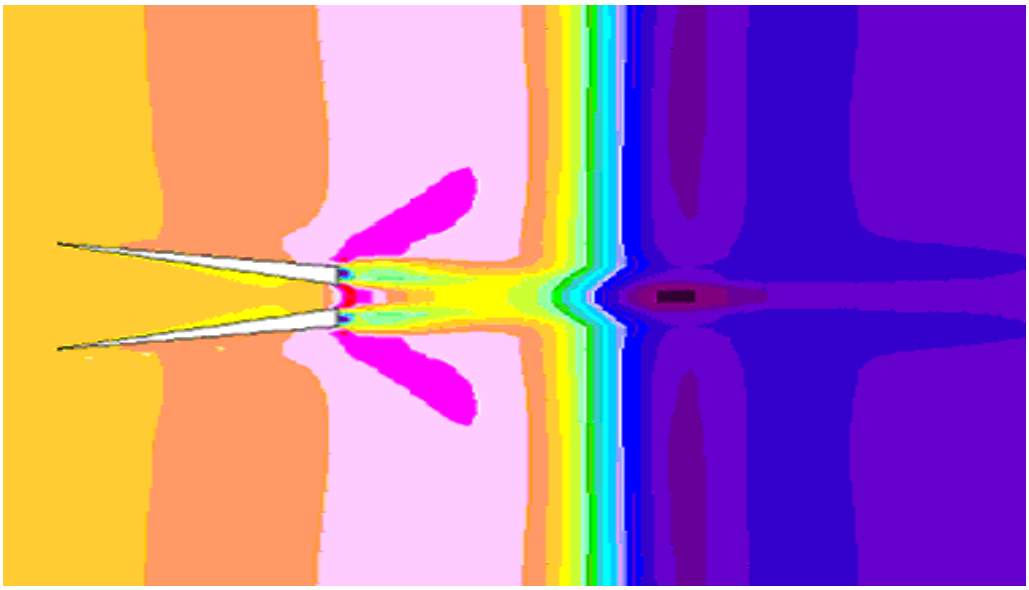

Fig. 11 . Velocity contour zoomed on the shock location zone at 0.0001/150(at the surface). The contour colour variation is as Fig.8.

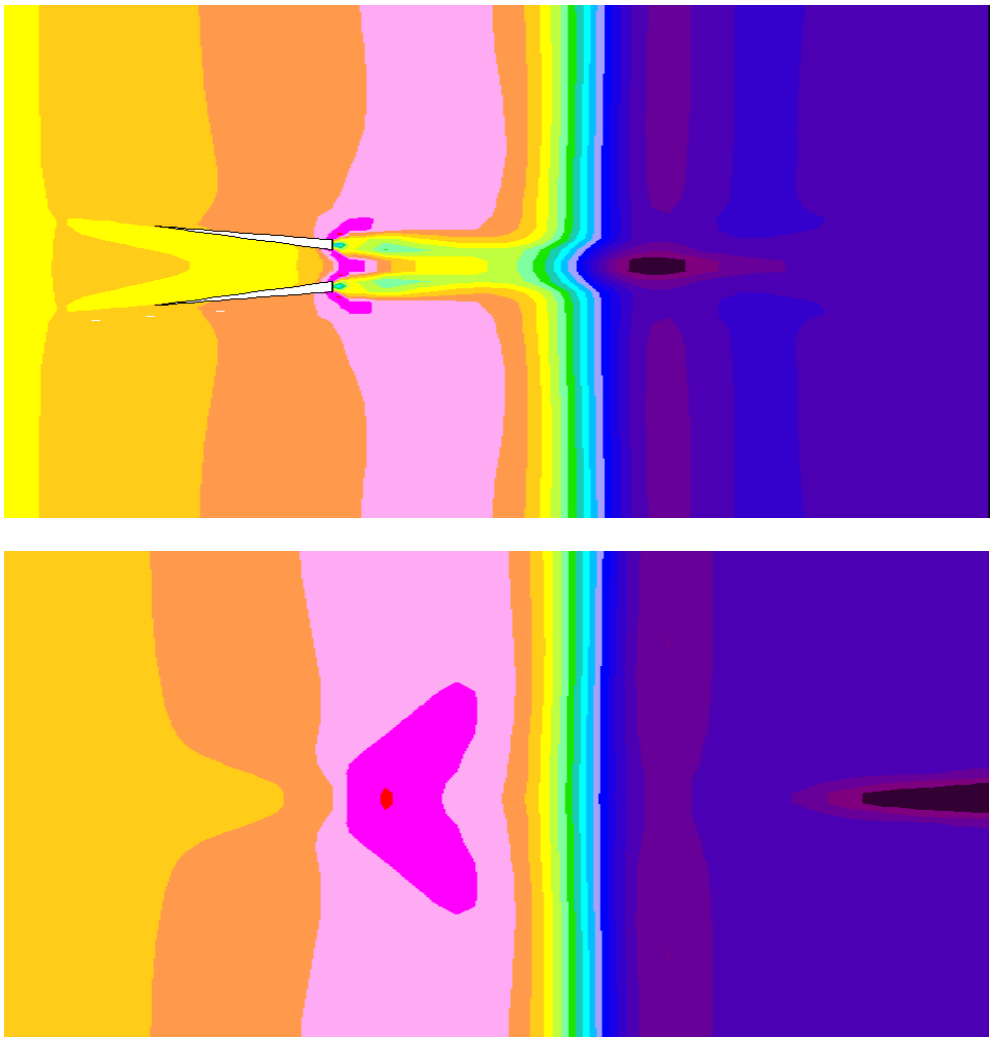

Fig. 12. Velocity contour zoomed on the shock location zone at 1mm (the top one) and 7 mm (the bottom one) above the surface. The contour colour variation is as Fig. C.8.

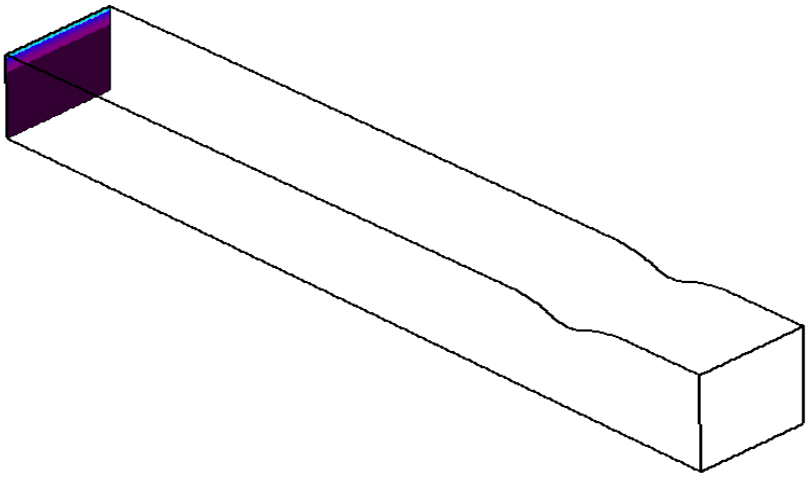

Fig. 13. Streamwise slice views through the wind tunnel

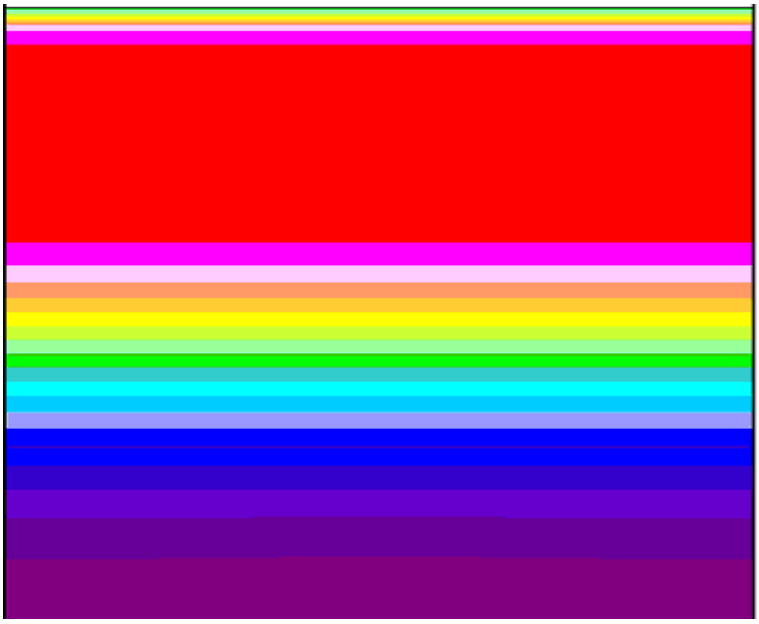

a) 10mm upstream of vortex generator leading edge (slice 50/860 mm)

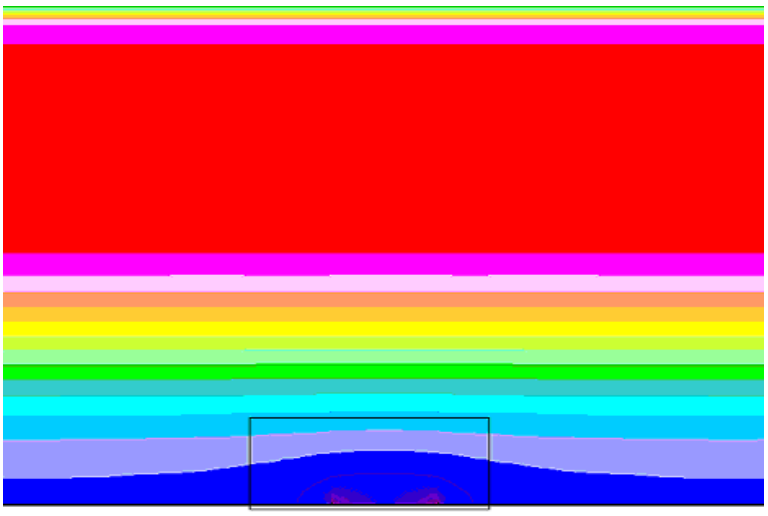

b) at vortex generator leading edge (60/860)

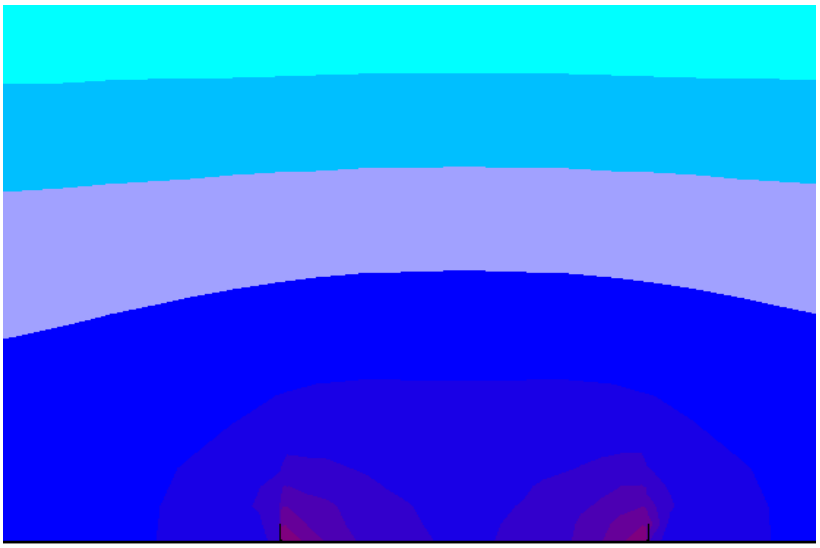

c) at vortex generator leading edge (60/860), zoomed at vortex area

Fig.14. Streamwise slices of velocity contour at the upstream and leading edge of vortex generator. The contour is as Fig.8.

Fig.15. Velocity contour for slice 89/860 (1mm to the trailing edge position, upstream shock location). The contour is as Fig.8.

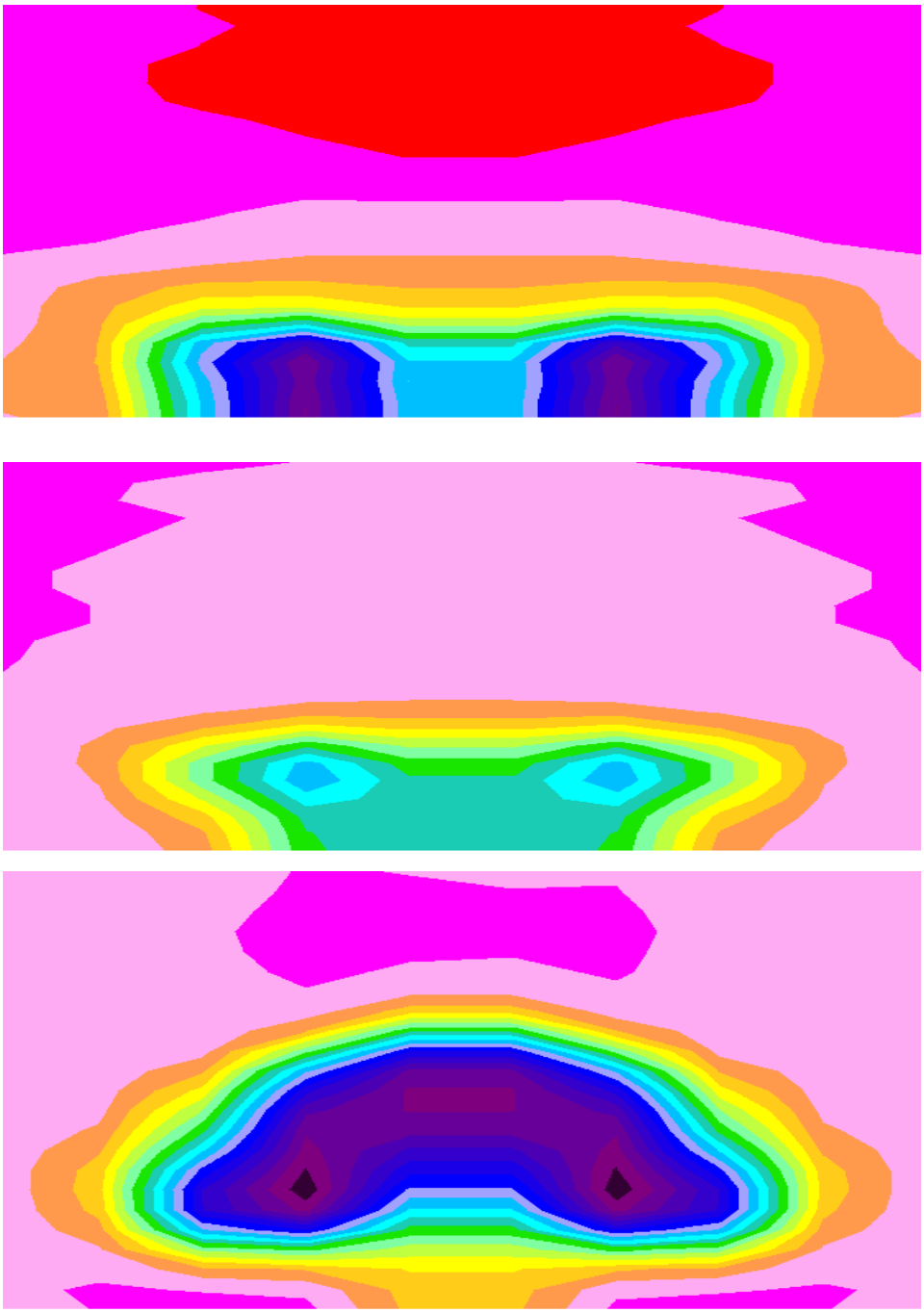

Fig. 16. Vortices formation downstream of vortex generator in velocity contour, streamwise from the top slice 100/860, 110/860 and 150/860, which are relatively 10mm, 20mm (2mm downstream shock wave) and 60mm downstream of vortex generator trailing edge. The contour is as Fig.8.

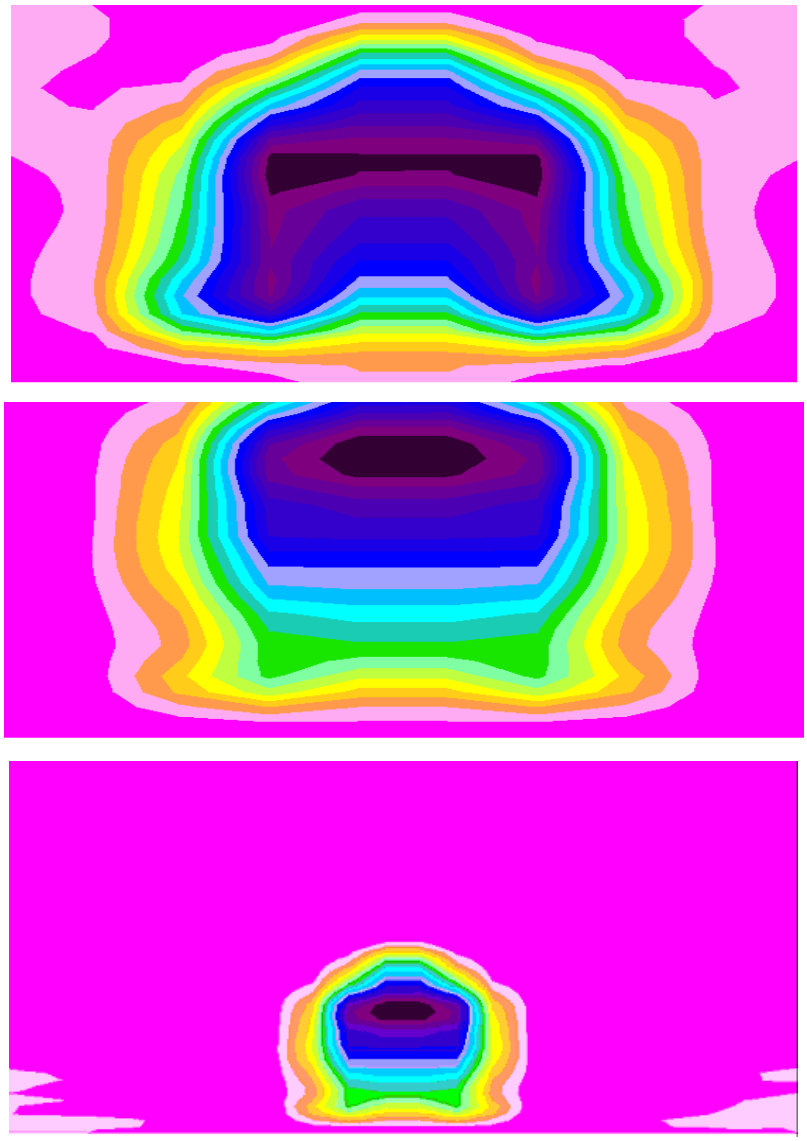

Fig.17. Merging the vortices in velocity contour: top slice 180/860 (90mm after vortex generator trailing edge), middle and bottom both are slice 230/860 (140 mm after trailing edge), middle is zoomed as before but bottom is the whole cross section of the wind tunnel. The contour is as Fig.8.

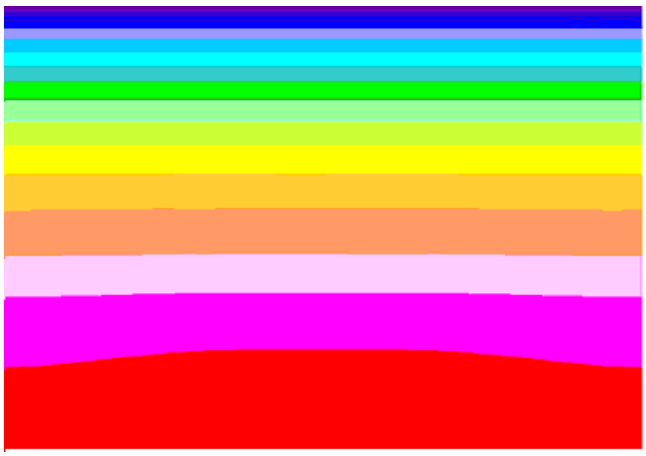

Fig. 18. Velocity contour at the full slice 630/860 (540 mm after vortex generator trailing edge and 400mm after shock wave location). The contour is as Fig.8.

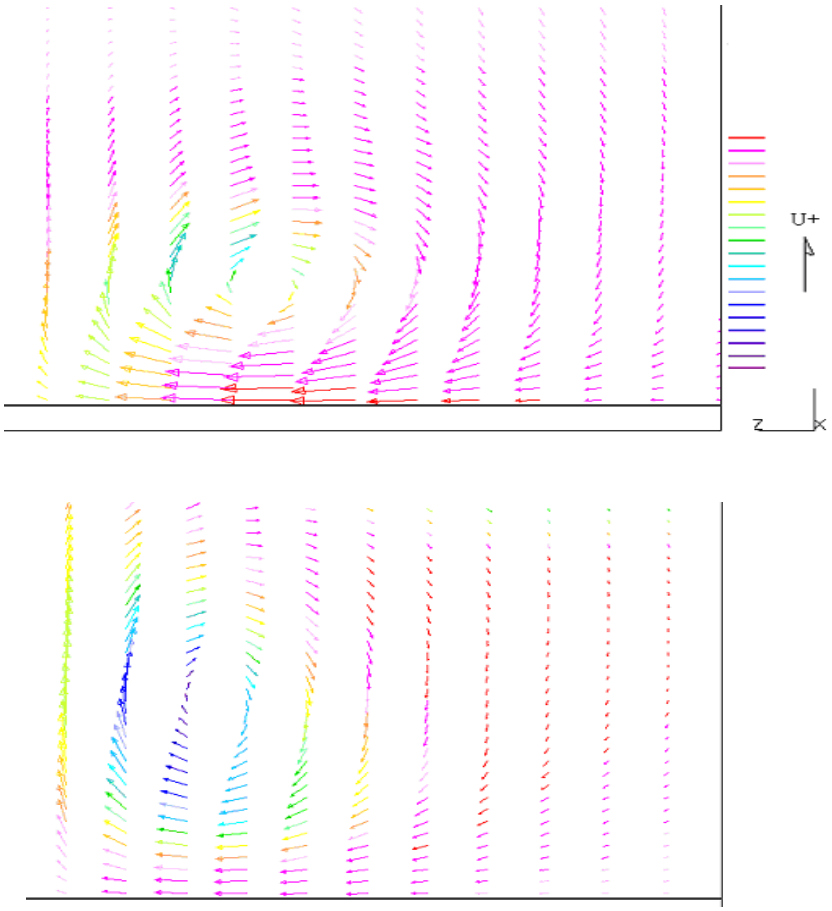

Fig. 19. Velocity vectors (v, w) around the generated flow near the surface; up: zoomed slice 100/860 (10mm downstream vortex generator trailing edge and 3mm upstream shock location); down: zoomed slice 120/860(13 mm downstream of shock location).

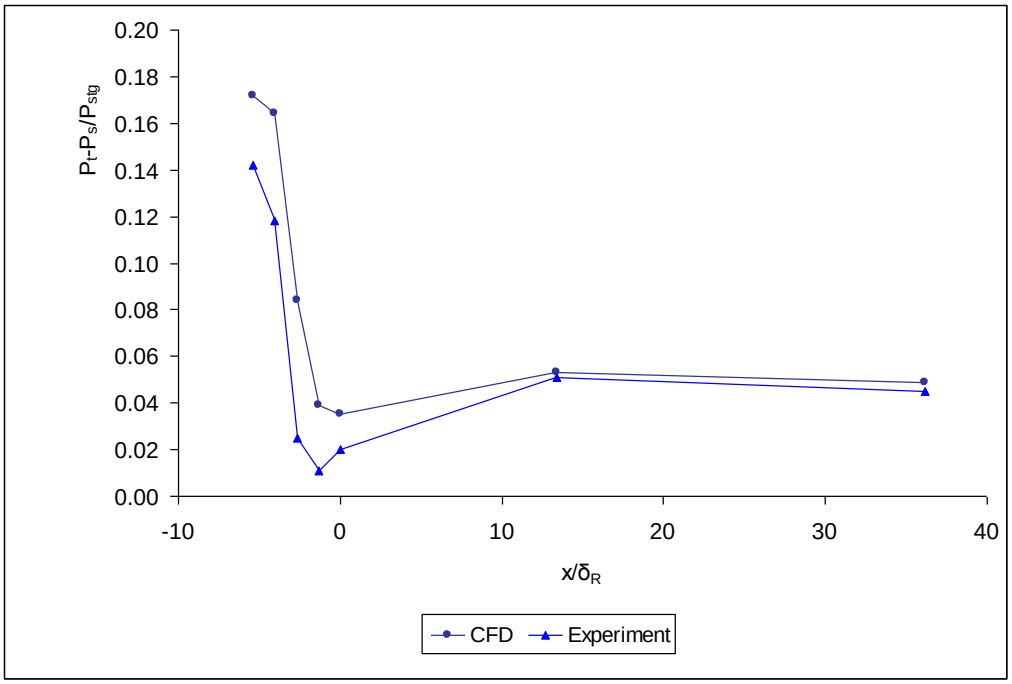

Fig.20. Distribution of experimental and CFD surface total pressure along the wind tunnel

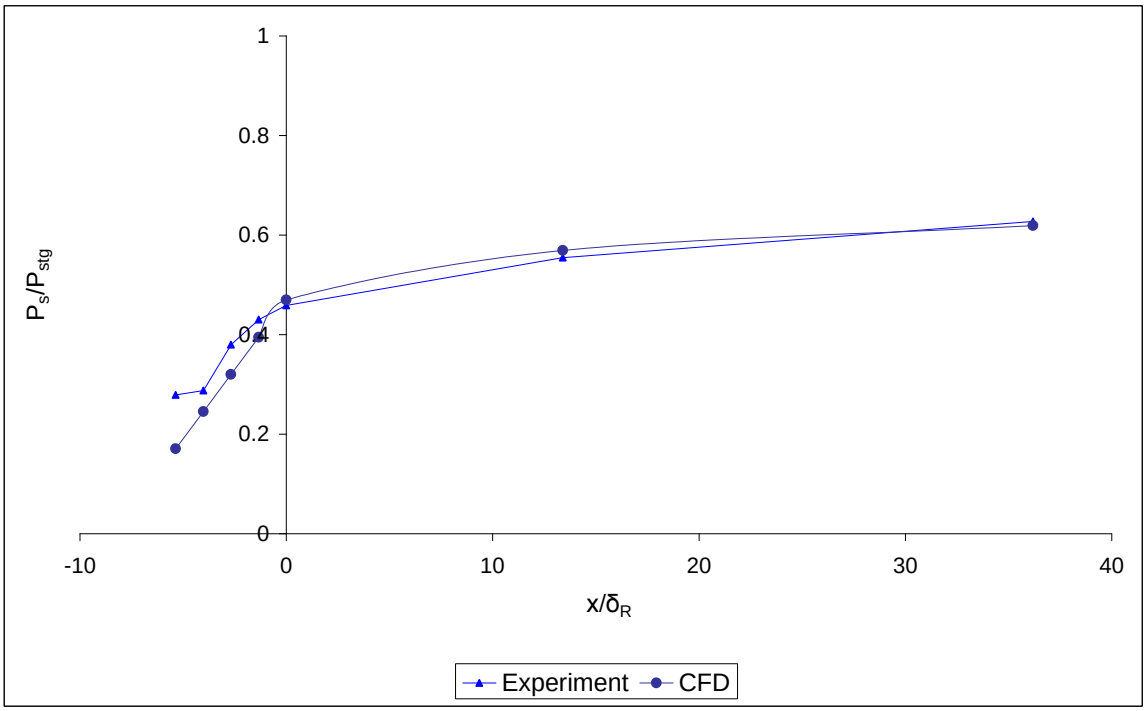

Fig.21. Static pressure distribution along the wind tunnel in experiment and CFD

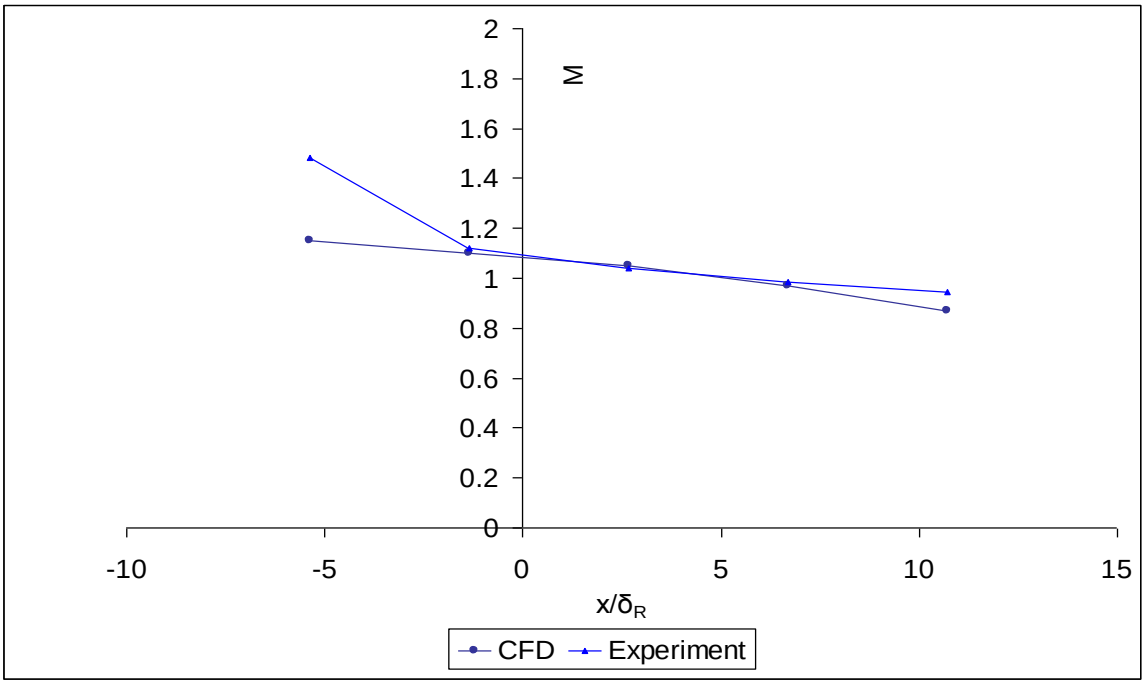

Fig. 22. Mach number in shock wave area for experiment and CFD

References

Zare Shahneh A., Motallebi F., "Effect of Submerged Vortex Generator on Shock Induced Separation in Transonic Flow" , QMU of London, AIAA, Journal of Aircraft, ISSN 0021-8669, JAIRAM, Vol. 46, pp. 856-863, 2009

Wng, Z.K., "A Source-Extraction Based Coupling Method for Computational Aeroacoustics", U. of Greenwich, 2003

Pierre Sagaut , "Large Eddy Simulation for Incompressible Flows", Springer,1998

Morkovin M.V. "Mecanique de la Turbulence", CNRS, pp.367-380 (1962)

Lesieur Marcel, Foreword for "Large Eddy Simulation for Incompressible Flows", 2000

Fluent Incorporated, 10 Cavendish Court, Lebanon, NH 03766-1442, 2005

Integrated Environmental Solution, 141 ST. James Road, Glassgow, G4 0LT

A. Kneer_ , E. Schreck_ , M. Hebenstreit_ , A. G¨oszler, Industrial mixed OpenMP / Mpi, ICCM Institute of Computational Continuum Mechanics GmbH, Hamburg, Germany

Aktin C. J., Squire L. C., " A Study of the Interaction of a Normal Shock Wave with a Turbulent Boundary Layer at Mach numbers between 1.3 and 1.55 ", European Journal of Mechanics, V. 11, No. 1, 1992

Jirasek A., "A vortex Generator Model and its Application to Flow Control", Swedish Defence Research Agency FOI, AIAA 2004-4965

STAR CD guide book

Methodology of STAR CD

PREPHA programme, "control of shock wave boundary layer interaction", S8 CH wind tunnel

Chakrabartty S. K., Dhanalakshmi K., Mathur J. S., "Computation of flow Past Aerospace Vehicles", National Aerospace Laboratories, Bangalore, India, 2005